



Open Access

Analysis of Spatial and Temporal Protein Expression in the Cerebral Cortex after Ischemia-Reperfusion Injury

Yuan-Hao Chen,^a Yung-Hsiao Chiang,^b Hsin-I Ma^a

^aDepartment of Neurological Surgery, Tri-Service General Hospital, National Defense Medical Center, Taipei, Taiwan, ROC

^bSection of Neurosurgery, Department of Surgery, Taipei Medical University Hospital, Taipei Medical University, Taipei, Taiwan, ROC

Received April 3, 2013
Revised September 24, 2013
Accepted September 26, 2013

Correspondence

Hsin-I Ma, MD, PhD
Department of Neurological Surgery,
Tri-Service General Hospital,
No. 325, 2nd Sec.,
Cheng-Kong Rd., Neihu Dist.,
Taipei 114, Taiwan, ROC
Tel +886-2-8792-7177
Fax +886-2-8792-7178
E-mail novamhi@gmail.com

Background and Purpose Hypoxia, or ischemia, is a common cause of neurological deficits in the elderly. This study elucidated the mechanisms underlying ischemia-induced brain injury that results in neurological sequelae.

Methods Cerebral ischemia was induced in male Sprague-Dawley rats by transient ligation of the left carotid artery followed by 60 min of hypoxia. A two-dimensional differential proteome analysis was performed using matrix-assisted laser desorption ionization-time-of-flight mass spectrometry to compare changes in protein expression on the lesioned side of the cortex relative to that on the contralateral side at 0, 6, and 24 h after ischemia.

Results The expressions of the following five proteins were up-regulated in the ipsilateral cortex at 24 h after ischemia-reperfusion injury compared to the contralateral (i.e., control) side: aconitase 2, neurotensin-related peptide, hypothetical protein XP-212759, 60-kDa heat-shock protein, and aldolase A. The expression of one protein, dynamin-1, was up-regulated only at the 6-h time point. The level of 78-kDa glucose-regulated protein precursor on the lesioned side of the cerebral cortex was found to be high initially, but then down-regulated by 24 h after the induction of ischemia-reperfusion injury. The expressions of several metabolic enzymes and translational factors were also perturbed soon after brain ischemia.

Conclusions These findings provide insights into the mechanisms underlying the neurodegenerative events that occur following cerebral ischemia. **J Clin Neurol 2014;10(2):84-93**

Key Words reperfusion injury, proteomics, protein expression, cerebral ischemia, neurodegenerative mechanisms, gerontology.

Introduction

A stroke is a major cerebrovascular event that can cause serious disability and even death. The protein expressions induced by stroke in affected brain regions during both the ictal and postictal stages remain a matter of controversy. The concept of proteomes was first introduced in 1995.¹ Since then, two-dimensional gel electrophoresis (2-DE) and mass spectrometry (MS) have been used widely to analyze thousands of proteins in individual experiments and to compare the overall protein

expressions of cells under different conditions.^{2,3} Several recent studies have investigated the alterations in protein expression relevant to various diseases, such as certain psychiatric disorders,⁴ Down's syndrome,⁵ Huntington's disease,⁶ and Alzheimer's disease.⁷ However, one study investigated the proteome of brain microdialysate obtained from the nonlesioned contralateral sides of the brains of three stroke patients.⁸

Focal brain infarcts are surrounded by extended perilesional zones that comprise the partially ischemic penumbra and nonischemic cortex referred to as the remote area. Little is known about protein expression in the penumbra and remote zones. Dynamic spatiotemporal patterns of gene induction after focal ischemia have been reported, and these patterns may contribute to the delayed progression of damage or, alternatively, may mediate neuroprotection, tissue remodeling, and

© This is an Open Access article distributed under the terms of the Creative Commons Attribution Non-Commercial License (<http://creativecommons.org/licenses/by-nc/3.0>) which permits unrestricted non-commercial use, distribution, and reproduction in any medium, provided the original work is properly cited.

functional compensation.⁹ In recent years there have been an increasing number of proteomics studies investigating the alterations in protein expression relevant to human diseases, but few of them have focused on strokes. Nonetheless, up-regulations of dihydropyrimidinase-related protein 2, spectrin alpha II chain, heat-shock cognate protein 70 pseudogene 1, and tropomodulin 2 have been found via MS after focal cerebral ischemia.¹⁰

The goal of the present study was to determine the protein profile in rat brains following experimental stroke induced by transient unilateral occlusion of the middle cerebral arteries (tMCAO). Identifying proteins with altered expression following a stroke may provide potential targets for neuroprotective therapy that would be of benefit to stroke patients. Fifty-eight protein spots with differential expression levels were found. Seven differentially expressed proteins were identified by matrix-assisted laser desorption ionization (MALDI)-time-of-flight (TOF) MS. These findings provide new clues regarding the mechanisms underlying transient ischemia and reperfusion injuries in cortical neurons.

Methods

Animals

Adult Sprague-Dawley rats ($n=12$) were anesthetized using chloral hydrate (400 mg/kg, i.p). All procedures were approved by the Institutional Animal Care and Use Committee of the National Defense Medical Center, and were compliant with the guidelines of the National Science Council on Animal Care.

MCA ligation

Temporary ischemia was induced by clipping the bilateral common carotid artery (CCA) and ligating the right-side middle cerebral artery (MCA), as suggested by Chen et al.¹¹ The bilateral CCA was isolated via a midline cervical incision, and then temporarily clipped with arterial clips. A right-side middle squamous craniotomy with a diameter of 2.0–3.0 mm was performed, and the MCA was ligated using a 10-0 suture. The suture was then released after 60 min of ligation, and the craniotomy site was covered with Gelfoam and bone wax. Individual animals were perfused intracardially at 0, 6, or 24 h ($n=3$ animals per time point) after ligation for reperfusion protein assay.¹²

Sample preparation

Animals were anesthetized and decapitated, and their brains then microdissected on ice under a surgical microscope to initially retrieve the cerebrocortices. The harvested brain tissue was cut into several 500- μm -thick sections. Punch separation of the cerebrocortex sections was then performed. The tissues

were homogenized on ice with a tissue tearer in 300 μL of sample buffer {58 mM dithiothreitol, 65 mmol/L 3-[(3-cholamidopropyl)dimethylammonio]-1-propanesulfonic, 7 M urea, 1.9 mol/L thiourea, 1.75% pH 3–10 carrier ampholytes}. The mixture was then mixed for 1 h and centrifuged at 18000 \times g for 10 min. Protein concentration was determined in the soluble supernatant using the RC-DC-Bio-Rad protein assay (Bio-Rad, Hercules, CA, USA) to avoid interference from ampholytes and reducing agents present in the buffer.

2-DE

A 2-DE system was used to separate proteins obtained from the cerebrocortex samples (250 μg /sample). An isoelectric focus over a pH range from 3 to 10 and a second dimension slab gel were used to separate the proteins by molecular weight while a first dimension gel was loaded on a large format (22 \times 22 cm). The gels were then stained using fluorescent SYPRO Ruby (Molecular Probes, Eugene, OR, USA) to quantify the proteins, and images were obtained using HT 2-D image analysis software (Genomic Solutions Inc., Ann Arbor, MI, USA).¹³

In-gel tryptic digestion

Samples were prepared using a modification of a previously described technique.¹⁴ Water (18 mol/L) was then used to wash the stained gel slabs extensively, excising the spot with a volume around 1–3 mm³. The gel pieces were mixed with ammonium bicarbonate (0.1 mol/L) to double the volume and then incubated at room temperature (20°C) for 15 min. The gel pieces were dried using a high-speed vacuum centrifuge after the solvent had been removed, rehydrated with 20 μL of 20 mmol/L dithiothreitol in 0.1 mol/L NH₄HCO₃, and then incubated at 56°C for 45 min to reduce the protein. When the tube was cooled to room temperature, the dithiothreitol solution was removed before 20 μL of 55 mmol/L iodoacetamide in 0.1 mol/L NH₄HCO₃ was added, and the gel incubated at room temperature in the dark for 30 min, followed by further incubation for 15 min in 0.2 mL of 50 mmol/L NH₄HCO₃, before adding 0.2 mL of acetonitrile. At the end of another 15-min incubation period at room temperature, the solvent was removed and the gel pieces were dried in a vacuum centrifuge. The gel pieces were rehydrated with 5 μL of 20 ng/ μL modified trypsin (Promega, Madison, WI, USA) in 50 mmol/L NH₄HCO₃ and then covered with 50 mmol/L NH₄HCO₃ solution and incubated overnight at 37°C.

Sample preparation for MALDI-TOF MS

A nitrocellulose solution was made by dissolving a nitrocellulose membrane in 1:1 acetone/isopropanol solvent. Alpha-cyano-4-hydroxycinnamic acid (-CN) was washed with 50 μL of acetone and the acetone phase was discarded. The -CN was

dissolved in acetone to a concentration of 10 mg/mL, and then the nitrocellulose and -CN solutions were mixed at a ratio of 1:4; 1 μ L of this mixture was deposited onto a 96-well MALDI target plate.

A sample was prepared for addition to the plate by adding 2 μ L of sample to 2 μ L of a solution of acetone-washed -CN dissolved in 0.1% trifluoroacetic acid and added to a 1:1 H₂O/acetonitrile mix to a final -CN concentration of 10 mg/mL. An aliquot (1 μ L) of the sample mixture was loaded onto each thin film. After the sample mixture was dried, 1.5 μ L of 2% formic acid in 18-M Ω water was added to each spot. The formic solution was removed by gentle blotting. This washing step was performed twice. The samples were then dried at room temperature. Fragment sizes were determined by MALDI-TOF MS.

Analysis of peptide sequences

Protein identification from tryptic fragment sizes was made using the Mascot search engine (www.matrixscience.com) based on the entire National Center for Biotechnology Information protein database under the assumptions that peptides are monoisotopic, oxidized at methionine residues, and carbamidomethylated at cysteine residues. Up to one missed trypsin cleavage was allowed, although most matches did not contain any missed cleavages. An accuracy of 100 ppm or greater for the tryptic sizes was required. The original protein size based on the portion of the gel from which the spot was excised was not restricted. All matches using mass values (either peptide masses or MS/MS fragment ion masses) were handled on a probabilistic basis. The total score is the probability that the observed match is a random event. The direct reporting of probabilities can be confusing, and so the probability-based molecular weight search score was used, defined as $-10 \times \log_{10}(p)$, where p is the absolute probability;¹⁵ thus, a probability of 10^{-20} becomes a score of 200. In this study, scores of >70 were considered significant ($p < 0.05$), and all protein identifications were in the expected size range based on their position in the gel.

Identification of differentially expressed proteins

Silver staining was performed using silver nitrate in combination with formaldehyde developer. The detection sensitivity of the silver stain was 0.5 ng. SYPRO-Ruby-stained gels were scanned using a high-resolution 12-bit camera and analyzed using HT 2-D gel software (Genomic Solutions). A composite gel was formed using gels obtained from each treatment. Bio-image software was initially used to identify matching spots in each tissue sample according to the manufacturer's instructions. The accuracy of the protein-spot matching was determined manually for each spot on each gel. The spot intensity was compared for each protein identified and matched, and

the integrated intensity of each spot was determined for each of the eight gels. Except where indicated otherwise, the data are presented as mean \pm SEM values, and a Mann-Whitney test was carried out on each to determine the significance of any differences.

Results

The true infarct volume obtained 24 h after tMCAO was 306.17 mm³ ($n=3$). Infarcted tissues were found predominantly on the lesioned sides of the cortices (Fig. 1). No infarctions were observed on the nonlesioned sides or in the sham-operated controls.

Two-dimensional gel electrophoresis maps were constructed for rat cortical proteins with or without tMCAO at pH 3–10. A typical 2-DE map of each group obtained from different cortical areas of the brain is shown in Fig. 2. After silver staining, about 400 spots in total were resolved in both maps and compared. There were no significant differences between the groups.

In addition to silver staining, SYPRO Ruby protein gel staining was performed to investigate the protein profile in the rat brain during the reperfusion stage following tMCAO. The 2-DE maps of sham-operated animals were compared at 6 and 24 h after tMCAO (Fig. 3). About 400 spots were found and histograms of each spot at different time points (0, 6, and 24 h following tMCAO) were compared (Fig. 4). The silver stain did not reveal significant up- or down-regulation of the protein profile, but the SYPRO Ruby stain revealed 8 spots of down-regulation and 39 spots of up-regulation at 24 h after reperfusion. On the other hand, 11 spots were up-regulated at 6 h and then returned to noninjury levels by 24 h. After in-gel digestion, the proteins were eluted from the spots and fingerprint patterns of peptides were prescribed by MALDI-TOF analy-

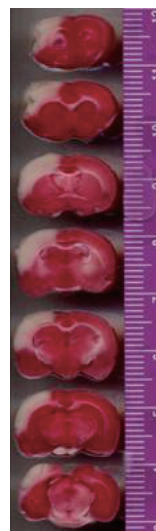


Fig. 1. Typical appearance of infarct areas in the rat brain at 24 h after transient occlusion of the middle cerebral artery. Normal tissues are stained purple with 2,3,5-triphenyltetrazolium chloride; infarcted tissue remains unstained. The appearance of this tissue relative to the sham-operated controls (data not shown) was similar to that of the nonlesioned contralateral hemispheres. The percentage volume of the hemispheric true infarct was typically 18–22%.

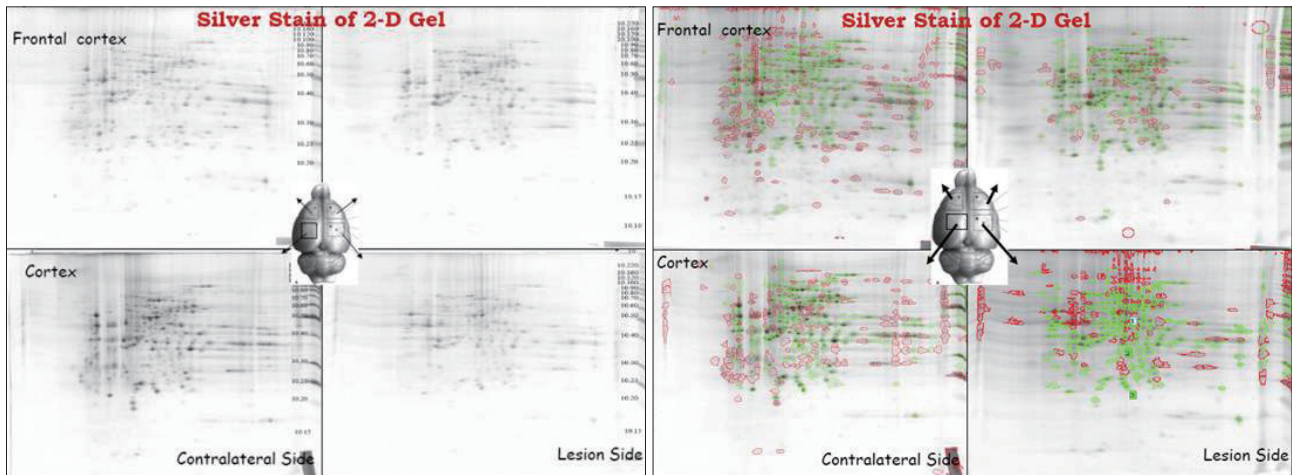


Fig. 2. Silver staining of 2-D gels of cerebrocortical tissue in different regions, revealing some different protein expression patterns.

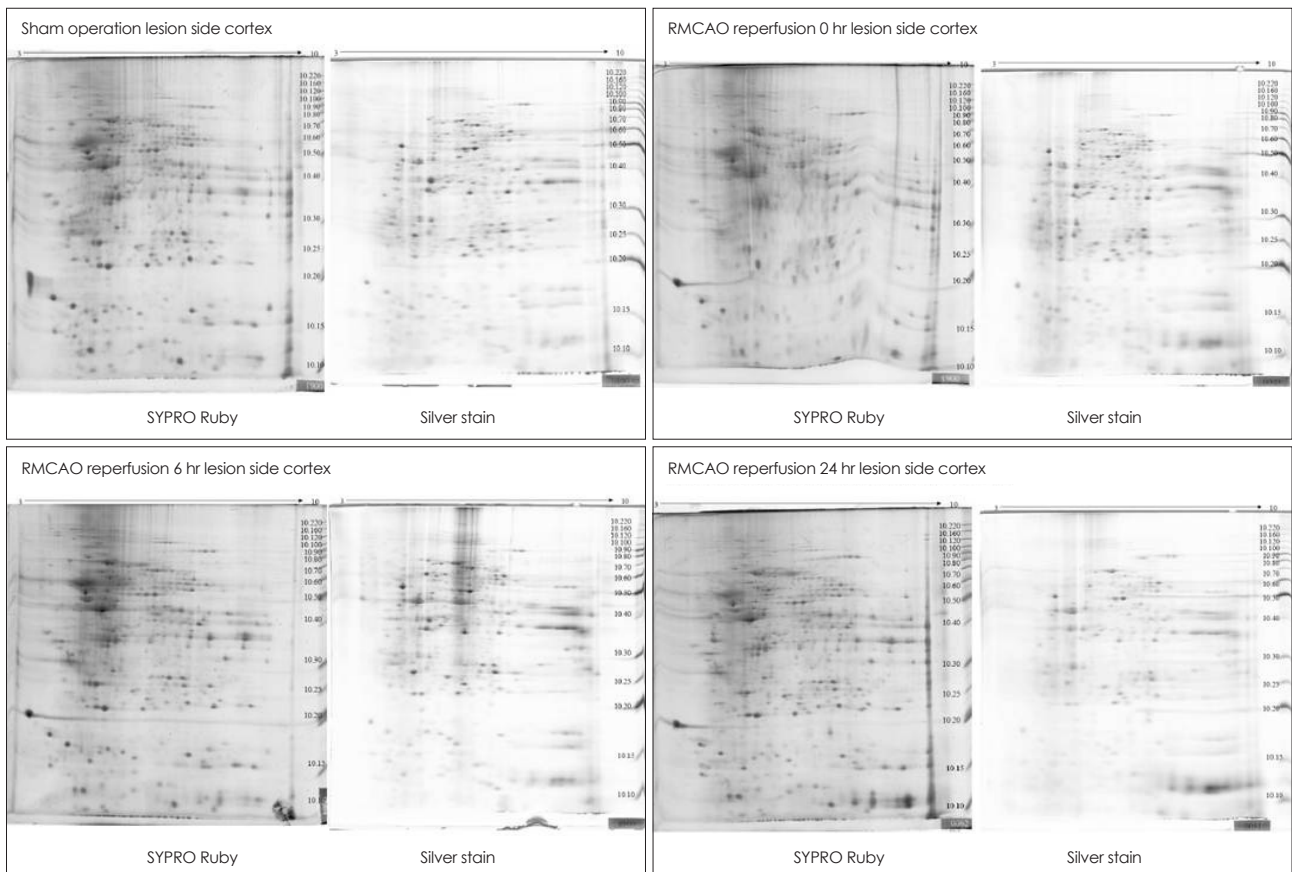


Fig. 3. Temporal proteomes of ischemia-reperfusion injury in the cerebrocortex: two types of stain (silver stain and SYPRO Ruby) were used on 2-D gels at various time points after ischemia-reperfusion injury.

sis. The proteins were identified after Mascot search comparison (Fig. 5). Of these, only seven were successfully identified by in-gel digestion by MALDI-TOF analysis, with a protein sequence coverage of 17–31% and top scores ranging from 62 to 111 (Table 1). Five spots were identified as aconitase 2, neurotensin-related peptide (NRP), hypothetical protein XP-212759, 60-kDa heat-shock protein (HSP60), and aldolase A.

The expression levels of these proteins were up-regulated by 1.43–5 times in comparison to their baseline expressions in the histograms. The observed molecular masses differed from the theoretical values by no more than 5–6%, and the observed isoelectric point values were also in close agreement with the theoretical values.

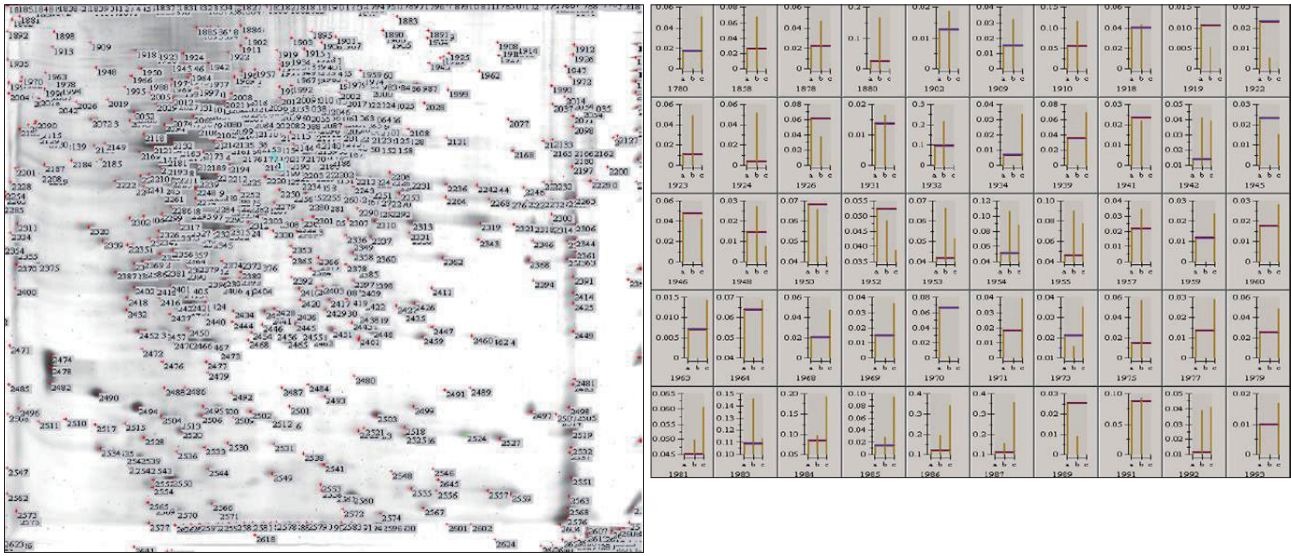


Fig. 4. Histogram comparing more than 400 spots to reveal pattern changes. SYPRO Ruby staining revealed 8 spots of down-regulated proteins and 39 spots of up-regulated proteins at 24 h after reperfusion. Conversely, 11 protein spots were up-regulated at 6 h and then returned to noninjury levels by 24 h.

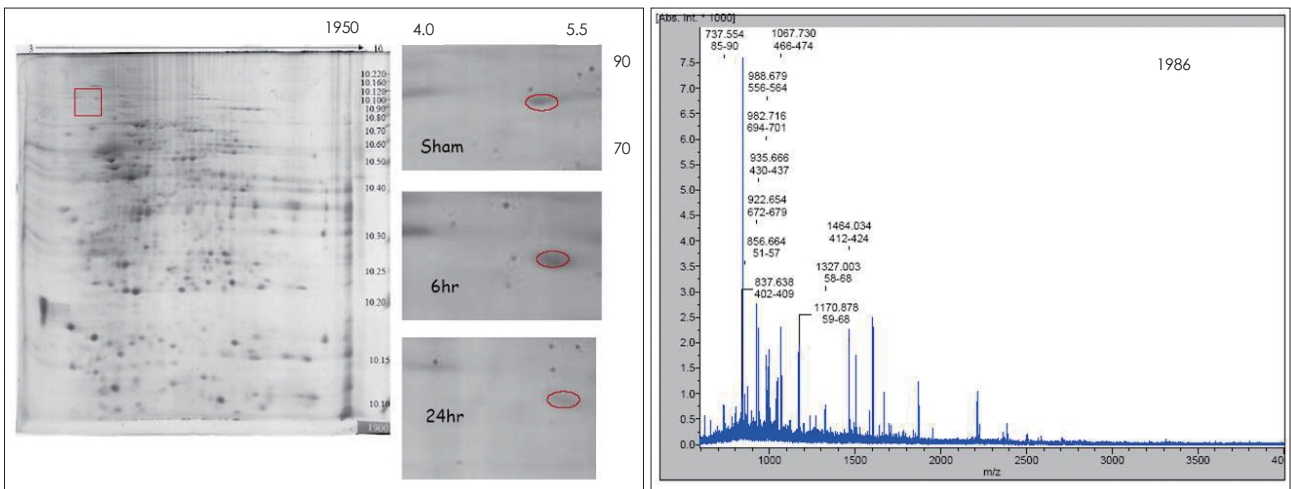


Fig. 5. After in-gel digestion, the protein was eluted from spot and fingerprint patterns of peptides and described using matrix-assisted laser desorption ionization-time-of-flight analysis. The proteins were identified by Mascot search comparison.

Discussion

To the best of our knowledge this is the first published analysis of the spatial and temporal expression of proteins from the cerebral cortex after ischemic stroke. Approximately 400 protein spots were resolved by 2-DE, and compared with sham-group samples. The silver staining did not show significant up- or down-regulation of the protein profile, but the SYPRO Ruby stain revealed 8 spots of proteins that were down-regulated and 39 spots of proteins that were up-regulated at 24 h after the reperfusion. It is perhaps somewhat surprising that only seven spots were identified. However, this should be seen in the context of the analyses having been done at a different time points, namely 0, 6, and 24 h, after tMCAO. Of the seven

protein spots that were identified, one was up-regulated at 6 h postischemia, five were up-regulated at 24 h postischemia, and one remained unidentified. The identified proteins are discussed individually below.

Protein up-regulation at 24 h after tMCAO

Aconitase 2

Aconitase is an iron-sulfur protein, or nonheme iron protein. Its iron-sulfur clusters are thought to play a role in the electron-transfer reactions of oxidative phosphorylation.¹⁶ The function of aconitase is to catalyze both steps so that isomerization of citrate is accomplished by a dehydration step followed by a hydration step in the citric acid cycle. The result is an inter-

Table 1. The biotechnology information and function of the identified spots containing proteins in cerebral cortex after ischemia-reperfusion

Spot no.	Identification	Function	NCBI/Swiss- Prot accession number	Top score*	Mr (Da)	pI	Relative change
Up-regulated at 24 h after reperfusion							
1986	Aconitase 2	Catalyzing enzyme in the citric acid cycle: nonheme iron protein	Gi 4053886	108	85380	7.87	2.92
2033	NRP		P02770	62	68674	6.09	5
2107	Hypothetical protein XP-212759		Gi 34875806	109	60967	5.91	1.43
2114	HSP60	Mitochondrial matrix protein	P63039	100	60917	5.91	3.5
2276	Aldolase A	Catalyzing enzyme in stage 2 of glycolysis	Gi 6978487	77	39783	8.31	5
Up-regulated at 6 h after reperfusion							
1954	Dynamin-1	GTP-binding protein; assembled around the neck of clathrin-coating pits	P21575	68	95867	6.32	2.2
Down-regulated at 24 h after reperfusion							
1950	GRP78	Immunoglobulin heavy-chain binding protein	P07823	111	72505	5.07	0.62

*A higher top score indicates a higher confidence in the identification.

change between a hydration atom and a hydroxyl group.

Mitochondria are the principal intracellular sources of superoxide (O_2^-) and hydrogen peroxide under both physiological and pathological conditions, and are therefore primary loci for reactions in these species and those derived from within their cells.¹⁷⁻¹⁹ Mitochondrial aconitase (m-aconitase), an enzyme that catalyzes the reversible isomerization of citrate and isocitrate via cis-aconitate in the Krebs cycle, contains a [4Fe-4S] prosthetic group in which one of the types of iron, Fe_{ox} , is not ligated to a protein residue, and can thus bind to hydroxyl groups of substrates or water.^{20,21} M-aconitase is highly sensitive to O_2^- -mediated inactivation; O_2^- selectively reacts at 10^7 /M/s with the iron-sulfur cluster, leading to the release of Fe_{ox} . M-aconitase is reactivated by the reincorporation of Fe^{2+} , which is facilitated by reductants such as glutathione. The ratio between [4Fe-4S]-aconitase and [3Fe-4S]-aconitase has been used to calculate the steady-state concentration of O_2^- in cells.²²

M-aconitase is a multifunctional protein: on the one hand it is a key enzyme for the Krebs cycle, while on the other hand it can act as a sensor in the redox regulation of metabolism by O_2^- .²³ The exquisite sensitivity of m-aconitase to inactivation by O_2^- may provide a control mechanism whereby decreasing the level of reducing equivalents (i.e., NADH) entering the electron transport chain would regulate the level of O_2^- produced by mitochondria.^{23,24}

Aconitase activity is also used in mitochondria activity assays. The mitochondrial activity in neurons increases to produce more ATP for cell repair-especially at the penumbra region-during the reperfusion state. On the other hand, increasing

the level of O_2^- after transient ischemia and reperfusion periods was found to suppress the activity of aconitase.²³ Aconitase may have created more for the energy requirements while their activity was being affected by higher levels of O_2^- . It can be speculated that the increase in aconitase enzyme levels found herein is due to increasing mitochondrial activity toward the production of more ATP for cell repair in the penumbra region.

NRP

Neurotensin is a tridecapeptide that is found within neurons in the brain and spinal cord, in endocrine cells in the pituitary gland and small intestine, and in chromaffin cells in the adrenal gland.²⁵ It is reported to have a broad spectrum of biologic effects, including effects on the endocrine, cardiovascular, digestive, and reticuloendothelial systems, as well as on temperature regulation, nociception, and behavior. Blood levels of immunoreactive neurotensin increase dramatically with the ingestion of food, and particularly fats. NRP releases histamine from mast cells and increases cutaneous vascular permeability; therefore, it might be speculated that NRP (or similar peptides) functions as an inflammatory mediator. In this regard, NRP could be formed locally in a manner similar to bradykinin, perhaps via the release or activation of acid protease activity, such as that of cathepsin D, and the second phase of inflammation is thought to be initiated by the release of lysosomal enzymes from phagocytes, elevating the acid protease activity in the skin during an inflammatory response.²⁶ The increases in NRP after the reperfusion period (24 h after tMCAO) in the present study may thus have been due to inflammation reac-

tions during the reperfusion state.

Hypothetical protein XP-212759

Hypothetical protein XP-212759 is an unknown protein that was identified in the present analysis. While bioinformatics tools have progressed remarkably, providing biologists with valuable information for functional elucidation, the prediction of protein function from sequences and structures remains difficult because homologous proteins often have different functions.²⁷ The existence of hypothetical proteins in genomes constitutes a major issue for comparative and functional genomics analyses. In particular for pathological conditions, these hypothetical proteins hamper the search for new and effective drug targets, and weaken progress in researching conditions such as strokes, rendering it difficult to improve our understanding of pathogenicity.²⁸

HSP60

The levels of HSP60 increased by around 3.5-fold at 24 h after ischemia in the penumbra region in this study; this protein was detected in both the cytoplasm and mitochondria. Purified cytoplasmic HSP60 exhibits chaperone activity, and the protein is imported into the mitochondria *in vitro* via a mitochondrial import assay. Under normal conditions, mammalian HSP60 is located both in the cytoplasm (as stable cytoplasmic HSP60) and in the mitochondria. Cytoplasmic HSP60 is rapidly imported into the mitochondria under severe conditions by cytoplasmic HSP70.²⁹ HSP60 and HSP10 are stress-inducible mitochondrial matrix proteins that form a chaperonin complex that is important for the folding and assembly of mitochondrial proteins. Simultaneous induction of the modified RNAs (mRNAs) for the mitochondrial chaperonins HSP60 and HSP10 in various regions in focal cerebral ischemia demonstrates that mitochondrial stress conditions persist concomitantly with cytosolic stress conditions in this state.³⁰ Furthermore, apoptosis is closely linked with mitochondrial dysfunction, which is involved in delayed neuronal death following brief periods of global cerebral ischemia,³¹ and this could be the reason why the protein was up-regulated at 24 h after the ischemia in the penumbra region.

Aldolase

Aldolase, an enzyme of the glycolytic pathway that catalyzes the aldol cleavage of fructose-1,6-biphosphate into glyceraldehyde-3-phosphate, was increased in the penumbra region by about fivefold in the present study at 24 h after ischemia. This enzyme is involved in the breakdown of glucose, fructose, and galactose, a process used by cells to generate energy in the form of ATP. Cell death after a stroke involves apoptotic, autophagocytic, and necrotic mechanisms that may cause the re-

lease of cytosolic proteins into the extracellular space. Release of aldolase into the extracellular space of the central nervous system has been found to take place in various disease states and in the presence of brain injury.³² The release of aldolase into the cerebrospinal fluid after stroke *in vivo*, as well as into the extracellular space after hypoxia in cell culture, has also been demonstrated.³³

Up-regulation of dynamin-1 at 6 h after reperfusion

Levels of dynamin-1 increased by about 2.2-fold at 6 h after ischemia in the penumbra region. The DTPase dynamin is required for late-stage endocytic clathrin-coated vesicle formation. Dynamin is targeted to coated pits on the plasma membrane in a guanine-nucleotide-independent manner, through interactions between its proline, arginine-rich COOH-terminal domain and the SH3-domain-containing protein amphiphysin. Mammals express three dynamins (dynamin-1, -2, and -3) with different expression patterns.³⁴ Dynamin-1 is expressed exclusively in the brain³⁵ and in neurons, and levels of dynamin-1 increase with synapse formation in parallel with the levels of synaptic vesicle proteins.³⁶ Furthermore, dynamin-1 plays a dedicated and essential role in the recycling of synaptic vesicles, which is critical to nervous system function.^{37,38} A late depolarizing postsynaptic potential induced by hippocampal CA1 pyramidal neurons after transient ischemia indicates an enhancement of synaptic transmission following ischemia.³⁹ The present data are compatible with those of reports indicating that synapse-releasing efficacy is increased during reperfusion periods.^{39,40}

Down-regulation of glucose-regulated protein 78-kDa (GRP78) at 24 h after reperfusion

The glucose-related stress response is part of a general cellular defense mechanism, referred to as the unfolded protein response (UPR), which is induced by glucose or oxygen starvation.^{41,42} One characteristic of the UPR is the induction of endoplasmic reticulum (ER) resident stress proteins, referred to as the glucose-regulated proteins (GRPs), which are Ca²⁺-binding chaperone proteins with protective properties.⁴³ The glucose-regulated protein GRP78, a 78-kDa protein (also referred to as binding immunoglobulin protein), is one of the best-characterized GRPs and is known to form complexes with heterologous proteins that are processed through the ER.⁴⁴ GRP78 can bind to misfolded proteins and unassembled complexes, and can protect cells against cell death caused by disturbances of the ER homeostasis.⁴⁵⁻⁴⁸ GRP78 has also been induced in endothelial cells damaged by reductive stress caused by hyperhomocysteinemia, which is a common risk factor for thrombotic vascular events such as premature arteriosclerosis, strokes,

myocardial infarctions, and thrombosis.^{49,50} Therefore, the induction of GRP could be an adaptive response that has evolved in mammals to protect endothelial cells against stress-induced death. GRPs are induced in response to stress, but once the stress is removed these proteins are posttranscriptionally modified into biologically inactive forms.⁴⁴ GRP78 is critical for the maintenance of cell homeostasis and the prevention of apoptosis. The present data show that this protein is present at very high levels at the beginning of the reperfusion period, or 1–6 h after tMCAO; however, as shown in Fig. 4B, it was relatively down-regulated at 24 h after reperfusion on the lesioned sides. This is probably the result of cell loss on the lesioned side relative to the contralateral side during the ischemic and reperfusion periods. In addition, the down-regulation of this molecular chaperone by tMCAO may indicate the potential for it to impact immune function on multiple levels.

Limitations and correlations

Matrix-assisted laser desorption ionization-time-of-flight mass spectrometry was used to evaluate the protein expression at various times after tMCAO. Sequence-similarity searches were conducted to enable proteomic analysis and comparison of proteins on the ischemic lesioned sides with those on the contralateral side at various time points in order to identify the protein changes during the postischemia period. The proteins that exhibited significant fluctuations included 1) the functional mitochondrial proteins, including HSP60 and aconitase; 2) NRP, the protein related to inflammation; 3) proteins associated with metabolism, including aldolase C and GRP78; 4) dynamin-1, which is involved in the release of synaptic neurotransmitters; and 5) one unknown hypothetical protein. These protein-level changes indicate the occurrence of changes in the systems involved in postischemic functional changes in the penumbra area.

There are also similar studies of brain ischemia that have described the following important protein level changes. First, functional changes in the pathways involving mitogen-activated protein and AKT kinase activity reflect the associated vulnerability to cerebrovascular injury. The alteration of gene and protein expression patterns, as well as the phosphorylation state of adenylyl-cyclase-associated protein 2, the so-called Turned On After Division-64 kDa protein, propionyl CoA carboxylase, APG-1, and valosin-containing protein (the kinase target) are consistent with the increased vulnerability of specific strains of animal (e.g., the spontaneously hypertensive stroke-prone rat) to cerebrovascular injury.⁵¹ Furthermore, stroke susceptibility was associated independently with multiple protein changes associated with ischemia, angiogenesis, or blood-brain barrier integrity. Aquaporin-4 and laminin- α -1 induction in cerebral cortical microvessels is associated with

stroke susceptibility. Significant molecular changes in ischemic cerebral microvasculature in the prestroke stage could contribute to the observed model phenotype of microhemorrhages and postischemic hemorrhagic transformation.⁵² Moreover, six plasma proteins, comprising α -2-macroglobulin, complement C3, inter- α -trypsin inhibitor heavy chain H3, serum albumin, haptoglobin, and transthyretin, which are classified as acute-phase proteins, changed significantly at 24-h postreperfusion after 90 min of left-MCA occlusion.⁵³ In addition, the analysis of the rat proteome in a study of the intestinal mucosa revealed that those proteins involved in the cellular processes of energy metabolism, antioxidation, and antiapoptosis changed by more than 1.5-fold following intestinal ischemia and reperfusion. Within these proteins, aldose reductase (AR) could remove reactive oxygen species, indicating that AR may play a key role in intestinal ischemic protection.⁵⁴

However, the data obtained in the present study were somewhat discrepant from those obtained in previous studies, which may have been due to the actual levels of verified proteins being lower than had been expected and because of poor sequence representations for proteomic identification by theoretical translation of publicly available data.⁵⁵ Overcoming the weakness of sequence-similarity searches requires consideration of several “similarity-free” methods,⁵⁶ including structural similarity searches looking for the global folding of the protein^{57–60} or detecting the functionally important regions of the protein.^{61–64} Thus, further experimentation is necessary to confirm the exact assignment of functions to the unknown protein.

Conflicts of Interest

The authors have no financial conflicts of interest.

Acknowledgements

This work was supported by the National Science Council, Taiwan under grant NSC98-2314-B016-016-MY2, and the Tri-Service General Hospital, Taiwan Medical Research Project grants TSGH-C100-033, TSGH-C101-084, and DOD96-37. We also appreciate the technical support and guidance for this study provided by Dr. Hao-Ai Shui, a professor at the Graduate Institute of Medical Sciences, National Defense Medical Center, Taipei, Taiwan, ROC.

REFERENCES

1. Swinbanks D. Government backs proteome proposal. *Nature* 1995; 378:653.
2. Hirano H, Kawasaki H, Sassa H. Two-dimensional gel electrophoresis using immobilized pH gradient tube gels. *Electrophoresis* 2000;21: 440–445.
3. Righetti PG, Castagna A. Recent trends in proteome analysis. *Adv Chromatogr* 2003;42:269–321.
4. Johnston-Wilson NL, Sims CD, Hofmann JP, Anderson L, Shore AD, Torrey EF, et al. Disease-specific alterations in frontal cortex brain proteins in schizophrenia, bipolar disorder, and major depressive disorder. The Stanley Neuropathology Consortium. *Mol Psychiatry* 2000;5:142–149.
5. Krapfenbauer K, Engidawork E, Cairns N, Fountoulakis M, Lubec G.

- Aberrant expression of peroxiredoxin subtypes in neurodegenerative disorders. *Brain Res* 2003;967:152-160.
6. Zabel C, Klose J. Influence of Huntington's disease on the human and mouse proteome. *Int Rev Neurobiol* 2004;61:241-283.
 7. Schonberger SJ, Edgar PF, Kydd R, Faull RL, Cooper GJ. Proteomic analysis of the brain in Alzheimer's disease: molecular phenotype of a complex disease process. *Proteomics* 2001;1:1519-1528.
 8. Maurer MH, Berger C, Wolf M, Fütterer CD, Feldmann RE Jr, Schwab S, et al. The proteome of human brain microdialysate. *Proteome Sci* 2003;1:7.
 9. Küry P, Schroeter M, Jander S. Transcriptional response to circumscribed cortical brain ischemia: spatiotemporal patterns in ischemic vs. remote non-ischemic cortex. *Eur J Neurosci* 2004;19:1708-1720.
 10. Chen A, Liao WP, Lu Q, Wong WS, Wong PT. Upregulation of dihydropyrimidinase-related protein 2, spectrin alpha II chain, heat shock cognate protein 70 pseudogene 1 and tropomodulin 2 after focal cerebral ischemia in rats—a proteomics approach. *Neurochem Int* 2007;50:1078-1086.
 11. Chen ST, Hsu CY, Hogan EL, Halushka PV, Linet OI, Yatsu FM. Thromboxane, prostacyclin, and leukotrienes in cerebral ischemia. *Neurology* 1986;36:466-470.
 12. Wang Y, Lin SZ, Chiou AL, Williams LR, Hoffer BJ. Glial cell line-derived neurotrophic factor protects against ischemia-induced injury in the cerebral cortex. *J Neurosci* 1997;17:4341-4348.
 13. Klein JB, Gozal D, Pierce WM, Thongboonkerd V, Scherzer JA, Sachleben LR, et al. Proteomic identification of a novel protein regulated in CA1 and CA3 hippocampal regions during intermittent hypoxia. *Respir Physiol Neurobiol* 2003;136:91-103.
 14. Ketritz R, Xu YX, Faass B, Klein JB, Müller EC, Otto A, et al. TNF-alpha-mediated neutrophil apoptosis involves Ly-GDI, a Rho GTPase regulator. *J Leukoc Biol* 2000;68:277-283.
 15. Pappin DJ. Peptide mass fingerprinting using MALDI-TOF mass spectrometry. *Methods Mol Biol* 1997;64:165-173.
 16. Berg F, Gustafson U, Andersson L. The uncoupling protein 1 gene (UCP1) is disrupted in the pig lineage: a genetic explanation for poor thermoregulation in piglets. *PLoS Genet* 2006;2:e129.
 17. Turrens JF, Boveris A. Generation of superoxide anion by the NADH dehydrogenase of bovine heart mitochondria. *Biochem J* 1980;191:421-427.
 18. Du Y, Miller CM, Kern TS. Hyperglycemia increases mitochondrial superoxide in retina and retinal cells. *Free Radic Biol Med* 2003;35:1491-1499.
 19. Turrens JF. Mitochondrial formation of reactive oxygen species. *J Physiol* 2003;552(Pt 2):335-344.
 20. Robbins AH, Stout CD. The structure of aconitase. *Proteins* 1989;5:289-312.
 21. Robbins AH, Stout CD. Structure of activated aconitase: formation of the [4Fe-4S] cluster in the crystal. *Proc Natl Acad Sci U S A* 1989;86:3639-3643.
 22. Hausladen A, Fridovich I. Superoxide and peroxynitrite inactivate aconitases, but nitric oxide does not. *J Biol Chem* 1994;269:29405-29408.
 23. Armstrong JS, Whiteman M, Yang H, Jones DP. The redox regulation of intermediary metabolism by a superoxide-aconitase rheostat. *Bioessays* 2004;26:894-900.
 24. Gardner PR, Fridovich I. Effect of glutathione on aconitase in *Escherichia coli*. *Arch Biochem Biophys* 1993;301:98-102.
 25. Uhl GR, Kuhar MJ, Snyder SH. Neurotensin: immunohistochemical localization in rat central nervous system. *Proc Natl Acad Sci U S A* 1977;74:4059-4063.
 26. Carraway RE, Mitra SP, Cochrane DE. Structure of a biologically active neurotensin-related peptide obtained from pepsin-treated albumin(s). *J Biol Chem* 1987;262:5968-5973.
 27. Park SJ, Son WS, Lee BJ. Structural analysis of hypothetical proteins from helicobacter pylori: an approach to estimate functions of unknown or hypothetical proteins. *Int J Mol Sci* 2012;13:7109-7137.
 28. Mazandu GK, Mulder NJ. Function prediction and analysis of mycobacterium tuberculosis hypothetical proteins. *Int J Mol Sci* 2012;13:7283-7302.
 29. Itoh H, Komatsuda A, Ohtani H, Wakui H, Imai H, Sawada K, et al. Mammalian HSP60 is quickly sorted into the mitochondria under conditions of dehydration. *Eur J Biochem* 2002;269:5931-5938.
 30. Izaki K, Kinouchi H, Watanabe K, Owada Y, Okubo A, Itoh H, et al. Induction of mitochondrial heat shock protein 60 and 10 mRNAs following transient focal cerebral ischemia in the rat. *Brain Res Mol Brain Res* 2001;88:14-25.
 31. Okubo A, Kinouchi H, Owada Y, Kunizuka H, Itoh H, Izaki K, et al. Simultaneous induction of mitochondrial heat shock protein mRNAs in rat forebrain ischemia. *Brain Res Mol Brain Res* 2000;84:127-134.
 32. Flórez G, Cabeza A, Gonzalez JM, Garcia J, Ucar S. Changes in serum and cerebrospinal fluid enzyme activity after head injury. *Acta Neurochir (Wien)* 1976;35:3-13.
 33. Linke S, Goertz P, Baader SL, Gieselmann V, Siebler M, Junghans U, et al. Aldolase C/zebrin II is released to the extracellular space after stroke and inhibits the network activity of cortical neurons. *Neurochem Res* 2006;31:1297-1303.
 34. Cook T, Mesa K, Urrutia R. Three dynamin-encoding genes are differentially expressed in developing rat brain. *J Neurochem* 1996;67:927-931.
 35. Cao H, Garcia F, McNiven MA. Differential distribution of dynamin isoforms in mammalian cells. *Mol Biol Cell* 1998;9:2595-2609.
 36. Ferguson SM, Brasnjo G, Hayashi M, Wölfel M, Collesi C, Giovedi S, et al. A selective activity-dependent requirement for dynamin 1 in synaptic vesicle endocytosis. *Science* 2007;316:570-574.
 37. Dikow AL, Lolova I, Ivanova A, Bojinov S. [Biochemical and histochemical studies of fructosephosphate aldolase in tumors of the nervous system. Isoenzymes of fructosephosphate aldolase. 8]. *Z Klin Chem Klin Biochem* 1969;7:606-613.
 38. Praefcke GJ, McMahan HT. The dynamin superfamily: universal membrane tubulation and fission molecules? *Nat Rev Mol Cell Biol* 2004;5:133-147.
 39. Gao TM, Xu ZC. In vivo intracellular demonstration of an ischemia-induced postsynaptic potential from CA1 pyramidal neurons in rat hippocampus. *Neuroscience* 1996;75:665-669.
 40. Gao TM, Pulsinelli WA, Xu ZC. Prolonged enhancement and depression of synaptic transmission in CA1 pyramidal neurons induced by transient forebrain ischemia in vivo. *Neuroscience* 1998;87:371-383.
 41. Lee AS. Coordinated regulation of a set of genes by glucose and calcium ionophores in mammalian cells. *Trends Biochem Sci* 1987;12:20-23.
 42. Kaufman RJ. Stress signaling from the lumen of the endoplasmic reticulum: coordination of gene transcriptional and translational controls. *Genes Dev* 1999;13:1211-1233.
 43. Lee AS. Mammalian stress response: induction of the glucose-regulated protein family. *Curr Opin Cell Biol* 1992;4:267-273.
 44. Little E, Ramakrishnan M, Roy B, Gazit G, Lee AS. The glucose-regulated proteins (GRP78 and GRP94): functions, gene regulation, and applications. *Crit Rev Eukaryot Gene Expr* 1994;4:1-18.
 45. Li LJ, Li X, Ferrario A, Rucker N, Liu ES, Wong S, et al. Establishment of a Chinese hamster ovary cell line that expresses grp78 anti-sense transcripts and suppresses A23187 induction of both GRP78 and GRP94. *J Cell Physiol* 1992;153:575-582.
 46. Yu Z, Luo H, Fu W, Mattson MP. The endoplasmic reticulum stress-responsive protein GRP78 protects neurons against excitotoxicity and apoptosis: suppression of oxidative stress and stabilization of calcium homeostasis. *Exp Neurol* 1999;155:302-314.
 47. Miyake H, Hara I, Arakawa S, Kamidono S. Stress protein GRP78 prevents apoptosis induced by calcium ionophore, ionomycin, but not by glycosylation inhibitor, tunicamycin, in human prostate cancer cells. *J Cell Biochem* 2000;77:396-408.

48. Reddy RK, Mao C, Baumeister P, Austin RC, Kaufman RJ, Lee AS. Endoplasmic reticulum chaperone protein GRP78 protects cells from apoptosis induced by topoisomerase inhibitors: role of ATP binding site in suppression of caspase-7 activation. *J Biol Chem* 2003;278:20915-20924.
49. Gazit G, Hung G, Chen X, Anderson WF, Lee AS. Use of the glucose starvation-inducible glucose-regulated protein 78 promoter in suicide gene therapy of murine fibrosarcoma. *Cancer Res* 1999;59:3100-3106.
50. Kokame K, Agarwala KL, Kato H, Miyata T. Herp, a new ubiquitin-like membrane protein induced by endoplasmic reticulum stress. *J Biol Chem* 2000;275:32846-32853.
51. Fornage M, Swank MW, Boerwinkle E, Doris PA. Gene expression profiling and functional proteomic analysis reveal perturbed kinase-mediated signaling in genetic stroke susceptibility. *Physiol Genomics* 2003;15:75-83.
52. Bergerat A, Decano J, Wu CJ, Choi H, Nesvizhskii AI, Moran AM, et al. Prestroke proteomic changes in cerebral microvessels in stroke-prone, transgenic[hCETP]-Hyperlipidemic, Dahl salt-sensitive hypertensive rats. *Mol Med* 2011;17:588-598.
53. Chen R, Vendrell I, Chen CP, Cash D, O'Toole KG, Williams SA, et al. Proteomic analysis of rat plasma following transient focal cerebral ischemia. *Biomark Med* 2011;5:837-846.
54. Liu KX, Li C, Li YS, Yuan BL, Xu M, Xia Z, et al. Proteomic analysis of intestinal ischemia/reperfusion injury and ischemic preconditioning in rats reveals the protective role of aldose reductase. *Proteomics* 2010;10:4463-4475.
55. Millares P, Lacourse EJ, Perally S, Ward DA, Prescott MC, Hodgkinson JE, et al. Proteomic profiling and protein identification by MALDI-TOF mass spectrometry in unsequenced parasitic nematodes. *PLoS One* 2012;7:e33590.
56. Kannan S, Hauth AM, Burger G. Function prediction of hypothetical proteins without sequence similarity to proteins of known function. *Protein Pept Lett* 2008;15:1107-1116.
57. Kawabata T, Nishikawa K. Protein structure comparison using the markov transition model of evolution. *Proteins* 2000;41:108-122.
58. Dundas J, Ouyang Z, Tseng J, Binkowski A, Turpaz Y, Liang J. CASTp: computed atlas of surface topography of proteins with structural and topographical mapping of functionally annotated residues. *Nucleic Acids Res* 2006;34(Web Server issue):W116-W118.
59. Holm L, Kääriäinen S, Rosenström P, Schenkel A. Searching protein structure databases with DaliLite v.3. *Bioinformatics* 2008;24:2780-2781.
60. Holm L, Rosenström P. Dali server: conservation mapping in 3D. *Nucleic Acids Res* 2010;38(Web Server issue):W545-W549.
61. Aloy P, Querol E, Aviles FX, Sternberg MJ. Automated structure-based prediction of functional sites in proteins: applications to assessing the validity of inheriting protein function from homology in genome annotation and to protein docking. *J Mol Biol* 2001;311:395-408.
62. Ondrechen MJ, Clifton JG, Ringe D. THEMATICS: a simple computational predictor of enzyme function from structure. *Proc Natl Acad Sci U S A* 2001;98:12473-12478.
63. Pazos F, Sternberg MJ. Automated prediction of protein function and detection of functional sites from structure. *Proc Natl Acad Sci U S A* 2004;101:14754-14759.
64. Nimrod G, Schushan M, Steinberg DM, Ben-Tal N. Detection of functionally important regions in "hypothetical proteins" of known structure. *Structure* 2008;16:1755-1763.